



24th DAAAM International Symposium on Intelligent Manufacturing and Automation, 2013

Robust Analysis of Stability in Internal Turning

Giovanni Totis^{*}, Marco Sortino

Department of Electrical, Management and Mechanical Engineering, University of Udine, Via delle Scienze 206, Udine 33100, ITALY

Abstract

When machining high precision mechanical parts, self-excited chatter vibrations must be absolutely avoided since they cause unacceptable surface finish and dimensional errors. Such unstable vibrational phenomena typically arise when the overall machining system stiffness is relatively low, as in the case of internal turning operations performed with slender boring bars. In general, it is not easy to determine stable tooling system configurations for a given machining operation, since data available in literature are often incomplete or inaccurate. In this paper, a new probabilistic algorithm for a robust analysis of stability in internal turning is presented. In this approach, model parameters are considered as random variables, and robust analysis of stability is carried out in order to estimate system's probability of instability for a given boring bar geometry and material, tool geometry, workpiece material and cutting parameters. By so doing, robustly stable tooling system configurations and cutting conditions may be identified in the preliminary production planning phase. The proposed approach was experimentally validated by considering different boring bar geometries and materials (including special boring bars made of high-damping carbide), tool geometries, workpiece materials and cutting conditions. For each machining system configuration, the developed approach was capable of successfully estimating the maximum ratio between boring bar overhang L and bar diameter D which assures process stability for most cutting parameters combinations.

© 2014 The Authors. Published by Elsevier Ltd. Open access under [CC BY-NC-ND license](https://creativecommons.org/licenses/by-nc-nd/4.0/).
Selection and peer-review under responsibility of DAAAM International Vienna

Keywords: internal turning; chatter prediction; robustness; tooling system

1. Introduction

When machining high-precision mechanical components, the static and dynamic behavior of the machining system during the cutting process plays a fundamental role, since it greatly affects the obtained surface quality. Basically, machining system vibrations can be split into the sum of forced and chatter vibrations.

^{*} Corresponding author. Tel.: +39-0432-558258; fax: +39-0432-558251.
E-mail address: giovanni.totis@uniud.it

Forced vibrations are generated during a regular cutting process and they cannot be completely avoided due to the compliance of the machining system.

However, their effect is usually small. On the contrary, chatter vibrations negatively affect part precision and surface quality, since they are unstable and chaotic. Also, they can cause abnormal tool wear, tool breakage, damage of the tooling structure and of the spindle bearings. For these reasons, avoidance of chatter vibrations is crucial.

Main physical mechanisms responsible for chatter in turning is the regenerative effect, deriving from the combination of the instantaneous tool-workpiece relative vibration with the waviness of machined surface left by the cutting tool at the previous round [1]. Regenerative chatter is dominant at medium-high spindle speeds. However, at low spindle speeds, rubbing of tool major flank against the machined surface – the so called process damping – tends to attenuate chatter vibrations, as recently confirmed by Altintas et al. [2].

Chatter prediction algorithms can be used for a preventive identification of stable machining system configurations [3][4][5]. Stability analysis of the cutting process requires accurate modeling of machining system dynamic behavior [6][7], cutting forces [8][9] and tool-workpiece dynamic interaction. In this manner, it is theoretically possible to forecast chatter onset dependencies on tooling system configuration, workpiece material and cutting parameters.

However, the methodologies proposed in literature are deterministic, i.e. their predictions are obtained from the nominal values of model coefficients. The possibly high uncertainties affecting model coefficients are neglected, although they may have a great impact on the stability analysis.

In this paper, a probabilistic approach is presented, which considers stochastic models for representing machining dynamics and tool-workpiece interaction. Main modal parameters as well as the regenerative radial force coefficient are considered as random variables. Their best guess values and probability density functions are calibrated by exploiting semi-analytical models based on the extensive experimental measurements presented in [10] and [11]. The model is finally experimentally validated, and main conclusions are drawn.

2. Internal turning dynamics

Tooling system is composed of several mechanical components, including the cutting insert, the boring bar and the toolholder, which is further fixed on lathe turret or machine tool head, as shown in Figure 1a). Finite Element modeling and experimental modal testing on such a tooling system are presented in [10] in great detail.

For most practical purposes it is sufficient to model the dynamic behavior along the radial direction, as proposed by Lazoglu et al. [6]. Accordingly, tool tip dynamic behavior along the radial direction will be only considered in the following treatment. Moreover, for most applications of industrial interest, tool tip dynamic compliance in the radial direction can be approximated as a single harmonic oscillator expressed in the form

$$W(j\omega) \approx \frac{G}{(j\omega/\omega_n)^2 + 2\zeta j\omega/\omega_n + 1} \quad (1)$$

where G is the total tool tip static compliance in the radial (x) direction, see Figure 1b), while ω_n and ζ are the natural pulsation and the damping coefficient associated to the main resonance peak, respectively.

In order to estimate the static compliance G , the model developed in [10] is adopted, as follows

$$G = \frac{L_{03}^3}{EJ} \left(\frac{1}{3} + \frac{\eta}{12} \right) + G_{u_{ot}} + H_{\varphi_{ot}} L_{03}^2 \quad (2)$$

where

- L_{03} is the sum of the nominal bar overhang $L=L_{13}$ and the additional bar overhang L_{01} which is necessary for describing the effect of imperfect cantilever constraint at node 1, see Figure 1c), in accordance with other authors [9][12];
- η is a small correction of Euler-Bernoulli model due to shear effects considered by the Timoshenko beam theory;
- J is the moment of inertia, while E is the Young's modulus of the considered boring bar material;

- G_{u0t} and $H_{\phi0t}$ are the translational and rotational static compliances modeling the static tool-holder behavior at node 0.

In the following, the static compliance G will be considered as a Gaussian random variable, with mean G_{best} given by Eq. (2) and with normalized random error $\varepsilon_G = \sigma_G / G_{best}$ ($\approx 10\%$) which should be assigned according to former experimental measurements or past experience.

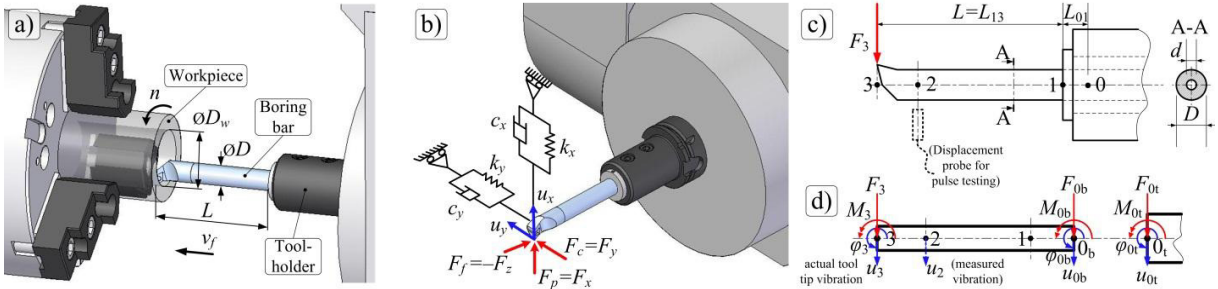


Fig. 1. a) General scheme of internal turning. b) Tooling system dynamics, represented by single harmonic oscillators acting along the radial (x) and tangential (y) directions. F_p is the back force component responsible for radial vibrations (u_x), whereas F_c is the main cutting force responsible for tangential vibrations (u_y). c) Schematic representation of the tooling system. d) Adopted FE model [10]

For estimating the damping coefficient ζ , the simple model tested in [10] was adopted

$$\zeta \cong \Lambda(L/D)\psi \tag{3}$$

where Λ and ψ are unknown empirical coefficients depending on boring bar material and clamping conditions, which have to be experimentally calibrated. In the following, damping ζ will be considered as a lognormal random variable, with mean ζ_{best} given by Eq. (3) and with normalized random error $\varepsilon_{\log \zeta} = \sigma_{\log \zeta} / \log \zeta_{best}$ ($\approx 20\%$) assigned according to experimental measurements or past experience. It should be noticed that static compliance models are generally accurate even when considering new conditions, whereas damping models may require re-calibration because it is very difficult to forecast damping properties for a new material.

3. Cutting force model

In this research work, a mechanistic cutting force model was adopted, see [13]. It is based on the assumption that the resultant cutting force acting on the tool is the sum of the infinitesimal contributions

$$\begin{cases} dF_c = k_{cs}dA(l) + k_{cp}dl \\ dF_n = k_{ns}dA(l) + k_{np}dl \end{cases} \tag{4}$$

where dF_c is the main cutting force, dF_n is the normal cutting force acting on the infinitesimal cutting edge dl , while dA is the infinitesimal uncut chip section area depending on the local uncut chip thickness $h(l)$, see Figure 2a). Shearing & Ploughing – S&P – cutting force coefficients were used to model the influence of dl and dA on the cutting force components. The influence of cutting speed v_c on S&P cutting force coefficients was neglected.

Cutting force components were obtained by integration along the cutting edge. In detail, the back force component F_p – which is mainly responsible for chatter vibrations – is given by

$$F_p = F_x = \int_0^B dF_n(l) \cos(\chi(l)) = k_{ns} \left[\int_0^B dA(l) \cos(\chi(l)) \right] + k_{np} \left[\int_0^B dl \cos(\chi(l)) \right] \tag{5}$$

It has to be pointed out that the total uncut chip section area A , the total length of contact B and the arguments between square brackets were computed numerically in order to take into account the effective shape of the uncut

chip section area, which can be very complicated, especially when feed f is of the same order of magnitude of nose radius r_ϵ . S&P cutting force coefficients have to be estimated experimentally or derived from literature, as illustrated in the next section.

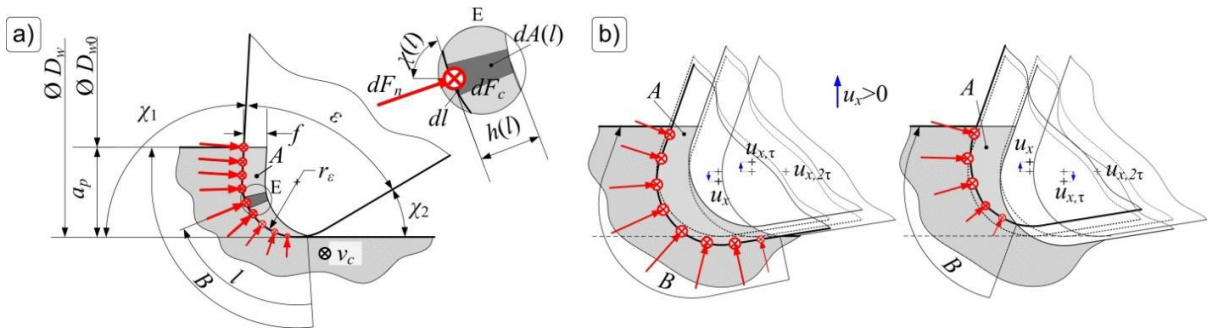


Fig. 2. a) Cutting force distribution along the cutting edge, depending on cutting edge geometry and cutting parameters, which determine the shape of the uncut chip section (of total area A and total contact length B). Local uncut chip thickness h depends on the curvilinear abscissa l , as well as the infinitesimal main cutting force (dF_c) and normal cutting force (dF_n) acting on the infinitesimal cutting edge dl . b) Influence of tool tip current vibration u_x and tool tip vibration at previous round $u_{x,\tau}$ on uncut chip section area A and workpiece – cutting edge contact length B . Tool tip vibration corresponding to two rounds before ($u_{x,2\tau}$) was set to zero, for the sake of simplicity. [11]

4. Cutter-workpiece dynamic interaction

Let τ be the spindle rotation period. Let us introduce the notation $u_{x,\tau}$ for representing the tool tip displacement one round before that currently considered, as illustrated in Figure 2b).

The radial back force F_x can be expressed as a function of the following independent variables

$$F_x \cong F_x(r_\epsilon, \chi_1, \chi_2, a_p, f, k_{ns}, k_{np}, u_x, u_{x,\tau}) \tag{6}$$

Let F_{x0} be the nominal radial back force corresponding to an ideal tooling system with infinite stiffness (no tool tip displacement, $u_x = u_{x,\tau} = 0$).

Let us suppose that the position of the real tooling system has been already corrected for compensating the static displacement caused by the nominal radial back force and by the finite static compliance G , i.e.

$$u_{x0} = u_{x,\tau 0} = GF_{x0} \tag{7}$$

Under these hypotheses, the equilibrium configuration is achieved when $u_x = u_{x,\tau} = 0$ and when the effective depth of cut a_p is equal to the nominal value. The variation of the radial back force δF_x due to tool tip vibrations u_x and $u_{x,\tau}$ can be determined as follows

$$\delta F_x = F_x - F_{x0} = \frac{\partial F_x}{\partial u_{x,\tau}} u_{x,\tau} + \frac{\partial F_x}{\partial u_x} u_x \approx \underbrace{\left(\frac{\partial F_x}{\partial u_{x,\tau}} \right)}_{k_\tau} (u_{x,\tau} - u_x) \tag{8}$$

where k_τ is the regenerative, radial cutting force coefficient, which has a strong influence on the stability of the cutting process [1][11].

Theoretical regenerative radial cutting force coefficient $k_{\tau,th}$ is usually computed by neglecting the influence of nose radius r_ϵ , since depth of cut a_p is supposed to be considerably greater than nose radius. Also, the feed f is generally assumed to be small in comparison with nose radius r_ϵ . Moreover, the calculation is carried out by considering infinitesimal vibrations du_x of the tool tip and by neglecting the variation of the radial back force due to the variation of the cutting edge contact length B . Under these hypotheses,

$$\delta F_x \cong k_{ns} \delta A \cos(\chi_1) = k_{ns} \frac{a_p}{\sin(\chi_1)} \underbrace{[\cos(\chi_1)(u_{x,\tau} - u_x)]}_{\delta h} \cos(\chi_1) \Rightarrow k_{\tau,th} \cong k_{ns} a_p \frac{(\cos(\chi_1))^2}{\sin(\chi_1)} \quad (9)$$

which is proportional to depth of cut a_p , the classical result of chatter theory. For a curvilinear cutting edge including a significant nose radius r_ε , under the hypothesis of a small feed to nose radius ratio and infinitesimal displacements, one obtains

$$k_{\tau,th} \cong k_{ns} \int_0^B [\cos(\chi(l))]^2 dl = k_{ns} \lambda \quad (10)$$

where the “form factor” λ is given by

$$\lambda = \begin{cases} r_\varepsilon \left[\frac{\sin(2\chi_{ap})}{4} + \frac{\chi_{ap}}{2} \right] & \text{if } a_p < a_{p,\chi_1} \\ r_\varepsilon \left[\frac{\sin(2\chi_1)}{4} + \frac{\chi_1}{2} \right] + \frac{(\cos(\chi_1))^2}{\sin(\chi_1)} (a_p - a_{p,\chi_1}) & \text{if } a_p \geq a_{p,\chi_1} \end{cases} \quad (11)$$

where

$$a_{p,\chi_1} = r_\varepsilon (1 - \cos(\chi_1)); \quad \chi_{ap} = \arccos\left(\frac{r_\varepsilon - a_p}{r_\varepsilon}\right) \quad \text{if } a_p < a_{p,\chi_1} \quad (12)$$

As a result, the theoretical regenerative radial cutting force coefficient $k_{\tau,th}$ depends on depth of cut a_p , nose radius r_ε , main working cutting edge angle χ_1 and shearing normal cutting force coefficient k_{ns} .

Nevertheless, in more general cutting conditions this simplified approach is not sufficiently accurate. In order to obtain better estimates, here a numerical approach was adopted, similar to that presented in [6], which is capable of taking into account the effect of non-zero nose radius r_ε , i.e. the effect of $a_p \approx r_\varepsilon$, together with realistic values of feed f (even when r_ε is small) and finite – i.e. non-infinitesimal – tool tip vibrations δu .

For this purpose, the following numerical procedure was conceived. For a given combination of main working cutting edge angle χ_1 , secondary working cutting edge angle χ_2 , nose radius r_ε , cutting parameters and cutting force coefficients, the nominal radial back force F_{x0} was first computed. A rectangular grid in the $(u_x, u_{x,\tau})$ plane, centered around the equilibrium condition (0,0) and composed 5×5 vertexes, was determined. Grid semi-amplitude was set equal to the static displacement estimated by Equation (7). The radial back force values corresponding to the selected couples $(u_x, u_{x,\tau})$ were computed. Eventually, the regenerative radial cutting force coefficient k_τ was estimated by linear regression performed on Equation (8).

Table 1. Numerical Design of Experiments for studying the regenerative, radial cutting force coefficient k_τ

Factor	Levels	Values
Main working cutting edge angle χ_1 [deg]	4	62.5, 75, 93, 107.5
Secondary working cutting edge angle χ_2 [deg]	4	5, 17.5, 32, 62.5
Nose radius r_ε [mm]	3	0.2, 0.4, 0.8
Depth of cut a_p [mm]	7	0.1, 0.2, 0.3, 0.4, 0.6, 0.8, 1.2
Feed f [mm/rev]	3	0.08, 0.12, 0.16, 0.20
Shearing normal cutting force coefficient k_{ns} [N/mm ²]	3	100, 400, 1600
Ploughing normal cutting force coefficient k_{np} [N/mm]	3	10, 40, 160
Tool tip static compliance G [$\mu\text{m}/\text{N}$]	2	0.25, 0.75

Calculation was repeated for each combination of factors' levels, according to the numerical Design of Experiments illustrated in Table 1. Analysis of variance was carried out (in logarithmic scale) in order to evaluate the influence of input factors on the output variable k_τ . When only main effects of input factors were considered, the outcome of the analysis was that all factors have a significant effect on the regenerative cutting force coefficient, see Table 2.

However, F -test values of working cutting edge angles χ_1 and χ_2 , as well as those of cutting parameters (a_p, f) and of static compliance G are practically negligible in comparison with F -test values of nose radius r_ϵ and of cutting force coefficients k_{ns} and k_{np} , which is partially in contrast with the classical theory. When two-factors interactions were included in the analysis, all main effects and factors' interactions proved to be significant, although the most important were those involving r_ϵ , k_{ns} and k_{np} .

By applying this "exact" numerical approach, some important sources of non-linearity affecting the radial force variation δF_p as a function of $(u_x, u_{x,\tau})$ can be highlighted. For instance, the effective shape of the uncut chip section A can be correctly identified, as well as the effective local uncut chip thickness $h(l)$, the latter being correctly set at zero when the regenerative contribution exceeds the static local value. On the contrary, in the linear classical approach this constraint is implicitly neglected. Similarly, the proposed approach correctly evaluates the variation of cutting edge contact length B , thus modeling the influence of the ploughing normal cutting force coefficient k_{np} , which is also neglected by the linear classical approach.

Table 2. Analysis of variance of regenerative radial cutting force coefficient k_τ with respect to considered input factors

Source	Sum Sq.	d. f.	Mean Sq.	F	Prob>F
χ_1	20.6	3	6.9	69.6	0
χ_2	564.6	3	188.2	1910.7	0
r_ϵ	2710.0	2	1355.0	13755.1	0
a_p	362.3	6	60.4	613.0	0
f	194.9	3	65.0	659.6	0
k_{ns}	7677.7	2	3838.9	38970.4	0
k_{np}	4833.8	2	2416.9	24535.1	0
G	129.2	1	129.2	1311.6	0
Error	2358.9	23946	0.1		
Total	18677.1	23968			

Therefore, the regenerative radial force coefficient derived from the numerical approach has to be interpreted as an approximate, average partial derivative $\partial F_p / \partial u_{x,\tau}$ computed within a domain of small but finite extension, which was determined by considering the static tool tip displacement due to the static back force F_{x0} as a reasonable reference amplitude for tool tip vibrations.

A first very rough model for estimating k_τ was expressed in the form of a constant times a power of the theoretical value $k_{\tau,th}$, yielding a poor square correlation coefficient $R^2=0.61$ (evaluated in natural scale). In addition, this model underestimates the effective value in 47% of cases, and the difference may be large. This may lead to imprudent decisions, since it may induce to consider a given machining system configuration as stable while it is on the contrary strongly unstable.

A more sophisticated model was built on main effects of most significant input factors (in logarithmic scale), i.e.

$$k_{\tau,mod} \approx 1.823 (\cos(\chi_2))^{0.261} r_\epsilon^{0.368} a_p^{0.097} f^{-0.263} k_{ns}^{0.496} \lambda^{0.287} k_{np}^{0.395} G^{-0.135} \quad (13)$$

where r_ϵ , a_p , f are expressed in [mm], k_{ns} in [N/mm²], k_{np} in [N/mm], G in [μ m/N]. This model is capable of describing the effective variability of k_τ with a slightly better square correlation coefficient $R^2=0.74$.

For achieving a more satisfactory interpolation, two-factor interactions have to be included in the model. In order to avoid overfitting, stepwise regression [14] was applied, yielding a model with 34 model coefficients whose performances are reported in Table 3 (model equation is not reported for the sake of brevity). This model describes k_τ variability with a good square correlation coefficient ($R^2=0.91$) and it is characterized by a small relative error E_{rel} between $k_{\tau,mod}$ and k_τ .

In short, in order to avoid the use of very complicated models, direct numerical computation is mostly recommended, whenever possible. Anyway, the estimate of k_τ depends on well-known quantities, such as tool geometry ($\chi_1, \chi_2, r_\epsilon$) and cutting parameters (a_p, f), and on generally unknown and uncertain physical quantities such as the normal shearing and ploughing force coefficients k_{ns} and k_{np} and the tool tip static compliance G .

Static compliance G can be estimated by using the model reported in section 2, and the effect of its uncertainty is limited because of the low sensitivity of k_τ to static compliance variations.

Table 3. Comparison between simple mathematical models approximating the radial cutting force coefficient k_τ .

Model description	$R^2(k_\tau, k_{\tau,mod})$	Standard deviation of E_{rel}	Mean of E_{rel}
Model based on theoretical regenerative radial force coefficient $k_{\tau,th}$	0.61	70%	18.2%
Model based on most relevant input factors and on theoretical form factor λ , Eq. (13)	0.74	35%	5.9%
Model based on most significant input factors (including form factor λ) and two-factor interactions (total of 1 constant plus 33 exponents estimated from linear regression performed in the logarithmic scale) selected by stepwise regression.	0.91	20%	2.0%

On the contrary, k_τ is strongly dependent on normal force coefficients k_{ns} and k_{np} , and the effect of their uncertainties cannot be neglected. Obviously, the most accurate estimates require direct cutting force measurements during several cutting tests, which can be rarely executed in a real industrial environment. Alternatively, first attempt estimates can be derived from workpiece supplier or tool manufacturer technical documentation, from machining databases and literature, in the simple form of the cutting pressure k_s , which is defined as the ratio of the main cutting force F_c to the uncut chip section area A . For a given cutting pressure k_s , Shearing and Ploughing coefficients are usually located in the following intervals

$$k_{cs} \approx (0.8 \pm 0.2)k_s; \quad k_{ns} \approx (0.45 \pm 0.3)k_{cs}; \quad k_{np} \approx (0.05 \pm 0.04)k_{cs}; \quad k_{cp} \approx (0.6 \pm 0.35)k_{np} \quad (14)$$

where the actual values may in general depend on the local geometry of cutting edge cross section (normal rake angle γ_n , normal clearance α_n , rounded cutting edge radius r_n and other details) and on the actual thermo-mechanical conditions at the chip – normal rake and machined surface – flank interfaces. For instance, slight variations of k_{cs} and k_{ns} may occur due to cutting speed variations, especially when machining light alloys in the high-speed range.

Accordingly, the regenerative radial force coefficient k_τ will be considered as a Gaussian random variable, with best guess value $k_{\tau,best}$ derived from numerical computation and normalized random error $\varepsilon_{k_\tau} = \sigma_{k_\tau} / k_{\tau,best} (\approx 20\%)$ dependent on the uncertainties affecting model coefficients.

5. Innovative robust stability analysis

For a given machining system configuration, which can be represented by its modal parameters (G, ω_n, ζ) , chatter occurrence does in general depend on spindle speed n and on the regenerative cutting force coefficient k_τ introduced in previous section. The (n, k_τ) plane can be split in two distinct regions, one stable and one unstable. In the standard chatter theory, depth of cut a_p is considered instead of the regenerative cutting force coefficient k_τ , since they are linearly correlated in the simplest case described by Eq. (9). The change of perspective proposed here is necessary because of the strong non-linearities of the function $k_\tau(a_p)$.

The borders separating the stable region from the unstable one are the so called stability lobes, as shown in Figure 3a). As reported in [1], the critical regenerative cutting force coefficient can be computed by the formula

$$k_{\tau,cr}(n) = -\frac{1}{2Re[W_x(j\omega_c(n))]} \quad (15)$$

where ω_c is the chatter pulsation associated to spindle speed n , yielding a negative real part of the frequency response (a positive real part would produce negative $k_{\tau,cr}$'s, which have no physical sense).

When the ratio of spindle rotation frequency ($n/60$) to the first natural frequency of the machining system $f_n = \omega_n / (2\pi)$ is relatively high (above 1/5, approximately), some stable cutting parameters can be found between adjacent lobes, which allow to enhance the material removal rate. On the contrary, for lower spindle speeds, stability lobes become too dense (as illustrated in Figure 3a)) and the only robustly stable region is that below the stability lobes minima, which can be determined by searching the maximum of the denominator of Eq. (15).

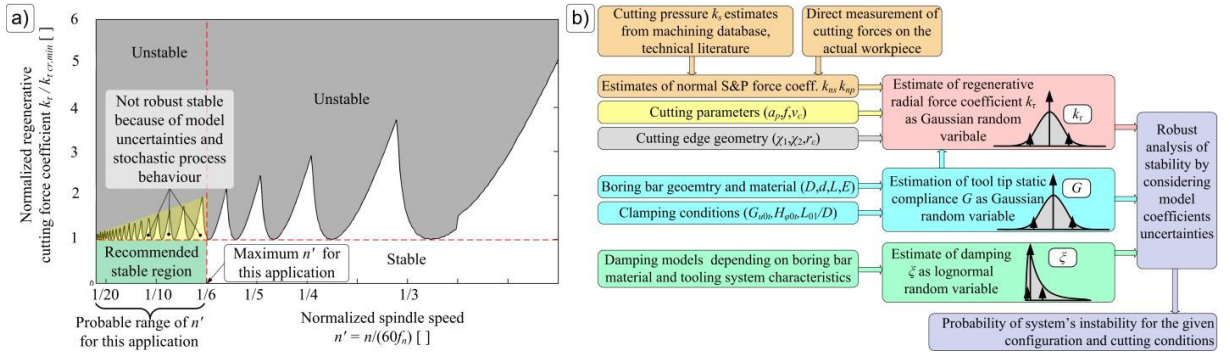


Fig. 3. a) Normalized stability lobe and b) general scheme of the proposed algorithm for robust analysis of stability

After some algebraic manipulations, the following result is obtained

$$k_{\tau} < k_{\tau,cr\ min} = \frac{2\xi(1 + \xi)}{G} \tag{16}$$

It can be noticed, Equation (16) is independent of the natural pulsation ω_n and of spindle speed n .

It has to be pointed out that process damping was neglected in this treatment (since this was the most conservative choice). However, process damping can be included in the model by introducing further stochastic coefficients, if necessary.

In the light of the subjects outlined in previous sections both members of Equation (16) have to be considered as random variables, whose statistical characteristics are assigned through the identification procedure, see Figure 3b).

Specifically,

- the tool tip static compliance is considered as an independent random variable normally distributed around its best estimate G_{best} , with normalized random errors ε_G such that the 95% confidence intervals is $G_{best}(1 \pm 2\varepsilon_G)$;
- the damping coefficient ξ is assumed lognormally distributed around its best estimate ξ_{best} , with normalized random errors $\varepsilon_{\log\xi}$ such that the 95% confidence interval (in logarithmic scale) is $\log\xi_{best}(1 \pm 2\varepsilon_{\log\xi})$;
- the regenerative radial cutting force coefficient k_{τ} is assumed as an independent random variable normally distributed around its best estimates $k_{\tau,best}$, with normalized random error $\varepsilon_{k_{\tau}}$ such that the 95% confidence interval is $k_{\tau,best}(1 \pm 2\varepsilon_{k_{\tau}})$.

System’s probability of instability for a given tooling system configuration, cutting tool, workpiece material and cutting conditions can be evaluated by applying the RCPM formula [15]

$$p_{instability} = \iiint \rho_d(k_{\tau}, G, \xi) p(k_{\tau}, G, \xi) dk_{\tau} dG d\xi \tag{17}$$

where ρ_d is equal to unity when Eq.(16) is satisfied and it is zero otherwise. The joint probability density function $p(k_{\tau}, G, \xi)$ can be easily expressed as

$$p(k_{\tau}, G, \xi) = p(k_{\tau})p(G)p(\xi) \tag{18}$$

since the considered random variables are assumed to be independent. By repeating this calculation for different tooling system configurations, cutting tool geometries and cutting conditions (workpiece material is supposed to be fixed by the considered machining application), it is possible to preliminarily optimize the cutting process.

6. Experimental validation

For validating the presented predictive approach, several cutting tests were carried out on a multifunction CNC lathe OKUMA Multus B300W, in dry conditions. Experimental tests were executed in three phases. In the first

phase, cutting force model coefficients of the selected workpiece materials were identified [11]. In the second phase, modal tests were executed on each tooling system configuration, in order to test and calibrate the mathematical models representing the tool tip static compliance (Eq.(2)) and the damping coefficient (Eq.(3)). In the third and last phase several cutting tests were performed in order to investigate the stability of the cutting process for different machining system configurations and cutting parameters combinations, as illustrated in Table 4.

Table 4. General Design of Experiments for chatter tests

Factor	Levels	Values
Boring bar material	2	Alloy steel: 42CrMo ($E=216\text{GPa}$, $A=6.52$, $\psi=-3.014$); High-damping carbide: Ni, Ta, W carbides + Co ($E=563\text{GPa}$, $A=12.66$, $\psi=-3.014$)
Boring bar diameter D [mm]	2	10 (with $d=4$), 16 (with $d=6$)
Workpiece material	2	C45 (213HB; $k_{ms}=1437\text{N/mm}^2$, $k_{np}=37.7\text{N/mm}$) ER GAL (151HB; $k_{ms}=117\text{N/mm}^2$, $k_{np}=32.8\text{N/mm}$)
Nose radius r_e [mm]	2	0.2, 0.4 0.2, 0.8 ($\chi_1=93^\circ$, $\chi_2=32^\circ$ for all inserts)
Aspect ratio L/D []	~ 4	$3 \div 9$
Depth of cut a_p []	4	0.1, 0.2, 0.4, 0.6
Spindle speed n [rpm]	9	4100 \div 4900

For each combination of boring bar type, cutting insert and workpiece material, different levels of the aspect ratio L/D were tested in the neighborhood of the expected critical value $(L/D)_{cr}$ which marked the transition from a completely stable to a completely unstable configuration. For a given L/D ratio, a dedicated Design of Experiments was carried out for evaluating process stability, involving different levels of depth of cut a_p and spindle speed n . Further technical details regarding experimental set-up and procedures can be found in [11]. On the average, 96 cutting tests were performed for each machining system configuration for a total of about 1600 cutting tests.

Both theoretical and experimental resonance frequencies confirmed the hypothesis that robust stable cutting conditions could be found only below stability lobes minima.

A machining system configuration was considered stable when at least 95% of the tested cutting parameters combinations were stable. Accordingly, the critical ratio $(L/D)_{cr,exp}$ was defined as the greatest stable L/D ratio.

A given tooling system configuration – determined by boring bar material and geometry, cutting tool nose radius and workpiece material was considered robust stable when the maximum probability of instability was smaller than 10% for all cutting parameters combinations. Accordingly, the predicted value $(L/D)_{cr,mod}$ was identified as the greatest L/D ratio such that this stability criterion was satisfied.

Table 5. Comparison between experimental and predicted values of $(L/D)_{cr}$

Boring bar material	Bar external diameter D [mm]	Workpiece material	Nose radius r_e [mm]	Exp. $(L/D)_{cr,exp}$	Predicted $(L/D)_{cr,mod}$	Relative error $E_{rel}\%$	$(L/D)_{max}$ recomm. by tool manufact.
Alloy steel	10	C45	0.2	4.5	4	-11	4
Alloy steel	10	C45	0.4	3.5	3.75	7	4
Alloy steel	10	ER GAL	0.2	5.5	4.75	-14	4
Alloy steel	10	ER GAL	0.8	4.25	4.25	0	4
Alloy steel	16	C45	0.2	5.25	4.25	-19	4
Alloy steel	16	C45	0.4	4.75	3.75	-21	4
Alloy steel	16	ER GAL	0.2	6	5	-17	4
Alloy steel	16	ER GAL	0.8	5.5	4.50	-18	4
High-damping carbide	10	C45	0.2	5.5	4.75	-14	6
High-damping carbide	10	C45	0.4	4.5	4.25	-6	6
High-damping carbide	10	ER GAL	0.2	6.5	5.75	-12	6
High-damping carbide	10	ER GAL	0.8	6	5.25	-13	6
High-damping carbide	16	C45	0.2	6.5	5	-23	6
High-damping carbide	16	C45	0.4	5.5	4.5	-18	6
High-damping carbide	16	ER GAL	0.2	7	6	-14	6
High-damping carbide	16	ER GAL	0.8	6.5	5.25	-19	6

For the numerical computations considered here, the following clamping conditions were assumed: $G_{rot}=0.023\mu\text{m/N}$, $H_{\phi 0r}=6.45\mu\text{rad/Nm}$, $L_{01}/D=0.7$ for all boring bars [10]. Moreover, the following normalized random errors were adopted: $\varepsilon_G=10\%$, $\varepsilon_{\log \zeta}=20\%$, $\varepsilon_{k\tau}=20\%$.

From the comparison between experimental results and predicted values of $(L/D)_{cr}$ reported in Table 5, it can be observed that the output is correctly underestimated in 94% of cases, with an average relative error of -13% and a standard deviation of relative error equal to 8%. Also, the proposed methodology is capable of explaining output variance with a satisfactory $R^2=0.83$. In addition, by comparison with maximum values of (L/D) suggested by tool manufacturer, it is worth noting that more reliable estimates can be obtained by applying the proposed methodology.

7. Conclusion

In this paper an innovative approach for robust chatter prediction in internal turning was presented.

The approach is based on the identification of machining system dynamics, represented by tool tip static compliance G and damping ζ , and on the identification of the regenerative radial cutting force coefficient k_r , representing the dynamic force interaction between cutting tool and workpiece during chatter vibrations. All these quantities are modeled as random variables with their own probability density functions. By so doing, the effects of model uncertainties and stochastic process behavior are taken into account when performing the stability analysis.

An innovative numerical procedure was applied to estimate the regenerative radial cutting force coefficient k_r . The comparison between the obtained numerical results and the estimates derived from classical analytical models evidenced large discrepancies, mainly due to the several sources of non-linearity which are neglected by the classical theory. It was assessed that k_r is mainly influenced by both normal Shearing & Ploughing coefficients k_{ns} and k_{np} , cutting edge geometry and cutting parameters, though the sensitivity to the depth of cut is relatively low, contrary to the usual conception. However, due to the high complexity of k_r as a function of the considered inputs, only regression models based on a large number of coefficients are capable of effectively representing its variability. Thus, a direct “exact” numerical approach is mostly recommended, whence the best guess value of k_r can be derived, together with its probability density function.

The method was successfully validated by comparing its predictions to the experimental results derived from a great variety of configurations, including different boring bar geometries and materials, cutting tool geometries and workpiece materials. The predictions proved to be in accordance with experimental results, thus allowing a preliminary robust selection of tooling systems assuring stable cutting conditions in internal turning operations.

References

- [1] Y. Altintas, E. Weck, *Chatter stability of metal cutting and grinding*, CIRP Annals – Manufacturing Technology, 53 (2004) 619–642.
- [2] Y. Altintas, M. Eynian, H. Onozuka, *Identification of dynamic cutting force coefficients and chatter stability with process damping*, CIRP Annals - Manufacturing Technology, 57 (2008) 371–374.
- [3] L. Vela-Martinez, J.C. Jauregui-Correa, E. Rubio-Cerda, *Analysis of compliance between the cutting tool and the workpiece on the stability of a turning process*, International Journal of Machine Tools & Manufacture, 48 (2008) 1054–1062.
- [4] R. Mahdavinjad, *Finite element analysis of machine and workpiece instability in turning*, International Journal of Machine Tools & Manufacture, 45 (2005) 753–760.
- [5] E. Budak, E. Ozlu, *Analytical modeling of chatter stability in turning and boring operations: multidimensional approach*, Annals of the CIRP, 53 (2007) 401–404.
- [6] I. Lazoglu, F. Atabey, Y. Altintas, *Dynamics of boring processes: Part III-time domain modeling*, International Journal of Machine Tools & Manufacture, 42 (2002) 1567–1576.
- [7] L. Andr n, L. Hakansson, A. Brandt, I. Claesson, *Identification of dynamic properties of boring bar vibrations in a continuous boring operation*, Mechanical System and Signal Processing, 18 (2004) 869–901.
- [8] B.C. Rao, Y.C. Shin, *A comprehensive dynamic cutting force model for chatter prediction in turning*, International Journal of Machine Tools & Manufacture, 39 (1999) 1631–1634.
- [9] B. Moetakef-Imani, N.Z. Yussefian, *Dynamic simulation of boring process*, International Journal of Machine Tools & Manufacture, 49 (2009) 1093–1103.
- [10] M. Sortino, G. Totis, F. Prospero, *Modeling the dynamic properties of conventional and high-damping boring bars*, Mechanical Systems and Signal Processing, 34 (2013) 340–352.
- [11] M. Sortino, G. Totis, F. Prospero, *Development of a practical model for selection of stable tooling system configurations in internal turning*, International Journal of Machine Tools & Manufacture, 61 (2012) 58–70.
- [12] L. Andr n, L.H. Akansson, A. Brandt, I. Claesson, *Identification of motion of cutting tool vibration in a continuous boring operation—correlation to structural properties*, Mechanical Systems and Signal Processing, 18 (2004) 903–927.
- [13] G. Totis, M. Sortino, *Development of a modular dynamometer for triaxial cutting force measurement in turning*, International Journal of Machine Tools & Manufacture, 51 (2011) 34–42.
- [14] S. Weisberg, *Applied linear regression*, Wiley Series in Probability and Statistics, 3rd edition, Wiley-Interscience, 2005.
- [15] G. Totis, *RCPM—A new method for robust chatter prediction in milling*, International Journal of Machine Tools & Manufacture, 49 (2009) 273–284.